The Ambisonics-Based Methods Implemented in the Chalmers Auralization Toolbox

Jens Ahrens

Technical note v. 2023/10/18

Chalmers University of Technology

jens.ahrens@chalmers.se

Abstract

This document presents a summary of those methods that are implemented in the Chalmers Auralization Toolbox[1] that perform auralization with an intermediate ambisonic representation. The documentation of the direct auralization approaches will be provided shortly.

1 Volumetric Sampling

Our implementation closely follows (Sheaffer et al., 2015) where volumetric sampling of the simulated sound pressure is performed for obtaining the spherical harmonic (SH) coefficients. We summarize this method in the following. (Sheaffer et al., 2015) may be considered an extension of (Støfringsdal and Svensson, 2006).

A sound pressure $S(\vec{\mathbf{x}}, \omega)$ at a point $\vec{\mathbf{x}}$ and at radian frequency ω can be represented by a sum of SH coefficients $\breve{S}_{n,m}(\omega)$ as (Gumerov and Duraiswami, 2005)

$$S(\vec{\mathbf{x}}, \omega) = \sum_{n=0}^{N} \sum_{m=-n}^{n} 4\pi \mathrm{i}^n \breve{S}_{n,m}(\omega)\, j_n\left(\omega \frac{r}{c}\right) Y_{n,m}(\beta, \alpha)\,. \tag{1}$$

$j_n(\cdot)$ denotes the spherical Bessel function of n-th order, and c denotes the speed of sound. The coordinate system is depicted in Fig. 1. The maximum order N of the decomposition in (1) is infinity for arbitrary sound fields but must be limited in the signal processing.

We use the following definition of the surface SHs $Y_{n,m}(\beta, \alpha)$, which is popular in the ambisonics community:

$$Y_{n,m}(\beta, \alpha) = (-1)^m \sqrt{\frac{2n+1}{4\pi} \frac{(n-|m|)!}{(n+|m|)!}}\, P_{n,|m|}(\cos\beta) \times \begin{cases} \sqrt{2}\sin|m|\alpha, & \forall m < 0 \\ 1 & , \forall m = 0 \\ \sqrt{2}\cos|m|\alpha, & \forall m > 0 \end{cases}. \tag{2}$$

$P_{n,m}(\cdot)$ are the associated Legendre polynomials (Gumerov and Duraiswami, 2005).

When sampling $S(\vec{\mathbf{x}}, \omega)$ volumetrically at Q points, (1) can be formulated separately for each sampling point $\vec{\mathbf{x}}_q$ ($q = 1, 2, \ldots Q$). The resulting set of equations can then be formulated for each angular frequency ω using matrix notation as

$$\mathbf{s} = \mathbf{B}\mathbf{s}_{\mathbf{n},\mathbf{m}}\,, \tag{3}$$

whereby $\mathbf{s}$ comprises the sampled sound pressure, $\mathbf{s} = [S(\vec{\mathbf{x}}_1, \omega)\ S(\vec{\mathbf{x}}_2, \omega)\ \ldots\ S(\vec{\mathbf{x}}_Q, \omega)]^T$, $\mathbf{B}$ is a $Q \times (N+1)^2$ matrix that contains the terms $4\pi \mathrm{i}^n j_n\left(\omega \frac{r_q}{c}\right) Y_{n,m}(\beta_q, \alpha_q)$ with q increasing downwards and (n, m) increasing towards the right according to the summation in (1), and $\mathbf{s}_{\mathbf{n},\mathbf{m}}$ contains the SH coefficients $\mathbf{s}_{\mathbf{n},\mathbf{m}} = [\breve{S}_{0,0}(\omega)\ \breve{S}_{1,-1}(\omega)\ \ldots\ \breve{S}_{N,N}(\omega)]^T$.

An estimate $\hat{\mathbf{s}}_{n,m}$ of $\mathbf{s}_{n,m}$ can be obtained from the sampled sound pressure $\mathbf{s}$ as

$$\hat{\mathbf{s}}_{n,m} = \mathbf{B}^{\dagger}\mathbf{s}\,, \tag{4}$$

[1] The Chalmers Auralization Toolbox is available here: https://github.com/AppliedAcousticsChalmers/auralization-toolbox

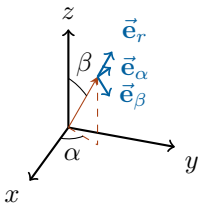

Figure 1: Spherical coordinate system with radius r, azimuth α, and colatitude β and their orientations $\vec{\mathbf{e}}_r$, $\vec{\mathbf{e}}_\alpha$, and $\vec{\mathbf{e}}_\beta$

whereby $\mathbf{B}^\dagger$ is the Moore-Pensore pseudoinverse of $\mathbf{B}$.

The Bessel functions $j_n\left(\omega\frac{r}{c}\right)$ in $\mathbf{B}$ exhibit zeros and take on very small values for small ω when $n > 0$. (Sheaffer et al., 2015) proposes soft-clipping for regularizing the problem, which limits how small the magnitude of the elements of $\mathbf{B}$ is permitted to be. It was originally proposed in (Bernschütz, 2016) for limiting the magnitude of a quantity and was reformulated in (Sheaffer et al., 2015) for the present purpose as $B_{\text{clipped}} = \left(\frac{2g}{\pi}\frac{|B|}{B}\arctan\frac{\pi}{2g|B|}\right)^{-1}$, whereby B is the quantity to be soft-clipped, and g is the minimum permitted magnitude on a linear scale after soft-clipping. This greatly improves the conditioning.

An SH representation of order N comprises $(N+1)^2$ SH coefficients $\breve{S}_{n,m}(\omega)$ that need to be deduced from the sampled sound pressure. Avoiding that the equation system in (3) is underdetermined requires at least $(N+1)^2$ sampling points.

2 Surface Sampling

The Kirchhoff-Helmholtz integral (Gumerov and Duraiswami, 2005) demonstrates that the sound pressure field inside a source-free domain is uniquely described by the sound pressure $S(\vec{\mathbf{x}},\omega)$ and normal sound pressure gradient $\frac{\partial}{\partial\vec{\mathbf{n}}}S(\vec{\mathbf{x}},\omega)$ distributions along the simply connected surface that encloses the domain. We therefore seek to establish a method that requires only sampling of that surface rather than inside the entire volume.

It is proven in (Burton and Miller, 1971, p. 207) that a weighted sum $S(\vec{\mathbf{x}},\omega) + \gamma\frac{\partial}{\partial\vec{\mathbf{n}}}S(\vec{\mathbf{x}},\omega)$ uniquely defines the sound pressure inside the volume that is enclosed by the surface so long as $\mathrm{Im}\{\gamma\} \neq 0$. We choose $\gamma = 1/(\mathrm{i}\frac{\omega}{c})$ here as this fulfills the uniqueness criterion, it assures that pressure and gradient are added with similar magnitudes, and it allows for the weighted sum to be interpreted as a virtual sensor with (far-field) cardioid directivity, which connects our formulation well to the literature on microphone arrays (Balmages and Rafaely, 2007; Thomas, 2019).

For ease of notation, we first formulate our proposed method for sampling points on a spherical surface that is centered around the coordinate origin and generalize the formulation to arbitrary surfaces in Sec. 2.2.

2.1 Spherical Surfaces

The signal $S_{\text{card.}}(\vec{x}_0,\omega)$ from a virtual sensor at position $\vec{\mathbf{x}}_0$ with frequency-independent far-field cardioid directivity facing outward in radial direction is obtained via (Balmages and Rafaely, 2007)

$$S_{\text{card.}}(\vec{\mathbf{x}}_0,\omega) = S(\vec{\mathbf{x}}_0,\omega) + \frac{1}{\mathrm{i}\frac{\omega}{c}}\frac{\partial}{\partial r}S(\vec{\mathbf{x}},\omega)\big|_{\vec{\mathbf{x}}=\vec{\mathbf{x}}_0}\,. \tag{5}$$

Sampling $S_{\text{card.}}(\vec{\mathbf{x}},\omega)$ along a spherical surface that is centered around the coordinate origin assures that the gradient in (5) is computed in outward-facing normal direction so that the uniqueness requirements are fulfilled. A similar case was treated in the literature on SMAs (Balmages and Rafaely, 2007; Thomas, 2019) and their 2-dimensional equivalent (Hulsebos et al., 2002) where the good conditioning was demonstrated. Using the equation of motion (Gumerov and Duraiswami, 2005, Eq. (1.1.3)), (5) can be expressed based on the normal particle velocity $V(\vec{\mathbf{x}},\omega)$ as

$$S_{\text{card.}}(\vec{\mathbf{x}}_0,\omega) = S(\vec{\mathbf{x}}_0,\omega) - \rho c\, V(\vec{\mathbf{x}}_0,\omega)\,, \tag{6}$$

whereby ρ is the mass density of air. In the following, we demonstrate how the equivalent to (3) can be formulated for this setting.

Expressing (5) in terms of SHs reads (Balmages and Rafaely, 2007)

$$S_{\text{card.}}(\vec{\mathbf{x}}_0,\omega) = \sum_n\sum_m 4\pi\mathrm{i}^n\breve{S}_{n,m}(\omega)\,\left[j_n\left(\omega\frac{r_0}{c}\right) - \mathrm{i}j_n'\left(\omega\frac{r_0}{c}\right)\right]Y_{n,m}(\beta_0,\alpha_0)\,. \tag{7}$$

Table 1: The components of (10). $P'_{n,|m|}(\cdot)$ is the derivative of $P_{n,|m|}(\cdot)$ with respect to the argument, which can be computed via a recurrence relation (Gumerov and Duraiswami, 2005, Eq. (2.1.53)).

$\frac{\partial}{\partial r} j_n\left(\omega \frac{r}{c}\right) = \frac{\omega}{c} j'_n\left(\omega \frac{r}{c}\right)$
$\frac{\partial}{\partial \beta} Y_{n,m}(\beta,\alpha) = (-1)^{m+1} \sqrt{\frac{2n+1}{4\pi} \frac{(n-\lvert m\rvert)!}{(n+\lvert m\rvert)!}}\, P'_{n,\lvert m\rvert}(\cos\beta) \sin\beta \begin{cases} \sqrt{2}\sin\lvert m\rvert\alpha, & \forall m < 0 \\ 1 & , \forall m = 0 \\ \sqrt{2}\cos\lvert m\rvert\alpha, & \forall m > 0 \end{cases}$
$\frac{\partial}{\partial \alpha} Y_{n,m}(\beta,\alpha) = (-1)^{m} \sqrt{\frac{2n+1}{4\pi} \frac{(n-\lvert m\rvert)!}{(n+\lvert m\rvert)!}}\, P_{n,\lvert m\rvert}(\cos\beta) \lvert m\rvert \begin{cases} \sqrt{2}\cos\lvert m\rvert\alpha, & \forall m < 0 \\ 0 & , \forall m = 0 \\ (-1)\sqrt{2}\sin\lvert m\rvert\alpha, & \forall m > 0 \end{cases}$

$j'_n(\cdot)$ is the derivative of $j_n(\cdot)$ with respect to the argument, which can be computed via a recurrence relation (Gumerov and Duraiswami, 2005, Eq. (2.1.87)). The equivalent of $\mathbf{B}$ in (3) now comprises all terms in the summation on the right hand side of (7) other than $\breve{S}_{n,m}(\omega)$. The equivalent of $\mathbf{s}$ comprises $S_{\text{card.}}(\vec{\mathbf{x}}_0, \omega)$, which we obtain from the simulated sound pressure according to (5) while approximating the gradient via the corresponding difference quotient as

$$\frac{\partial}{\partial r} S(\vec{\mathbf{x}}, \omega)\Big|_{\vec{\mathbf{x}}=\vec{\mathbf{x}}_0} = \frac{S(\vec{\mathbf{x}}_2, \omega) - S(\vec{\mathbf{x}}_1, \omega)}{\|\vec{\mathbf{x}}_2 - \vec{\mathbf{x}}_1\|}\,, \tag{8}$$

which we can compute directly from the simulation data. $\vec{\mathbf{x}}_0 = \frac{\vec{\mathbf{x}}_2 - \vec{\mathbf{x}}_1}{2}$ is the midpoint between $\vec{\mathbf{x}}_1$ and $\vec{\mathbf{x}}_2$, which have to lie accordingly on a radial line.

2.2 Arbitrary Surfaces

As the uniqueness criterion $\mathrm{Im}\{\gamma\} \neq 0$ from (Burton and Miller, 1971) holds for arbitrary simply-connected surfaces, we generalize the formulation from Sec. 2.1 here and establish the equivalents of (5) and (7) – and consequently of (3) and (4) – for such arbitrary surface shapes.

We need to compute the gradient in direction $\vec{\mathbf{n}} = \vec{\mathbf{n}}(\vec{\mathbf{x}}_0)$ that is normal to the arbitrary surface at the point $\vec{\mathbf{x}}_0$. The partial derivative with respect to r in (5) needs to be replaced with the derivative in direction of the unit-length vector $\vec{\mathbf{n}}$ (pointing in direction $(\beta_{\vec{\mathbf{n}}}, \alpha_{\vec{\mathbf{n}}})$), which is given by

$$\frac{\partial}{\partial \vec{\mathbf{n}}} S(\vec{\mathbf{x}}, \omega)\Big|_{\vec{\mathbf{x}}=\vec{\mathbf{x}}_0} = \begin{bmatrix} \cos\alpha_{\vec{\mathbf{n}}} \sin\beta_{\vec{\mathbf{n}}} \\ \sin\alpha_{\vec{\mathbf{n}}} \sin\beta_{\vec{\mathbf{n}}} \\ \cos\beta_{\vec{\mathbf{n}}} \end{bmatrix}^T \nabla\, S(\vec{\mathbf{x}}, \omega)\Big|_{\vec{\mathbf{x}}=\vec{\mathbf{x}}_0} \tag{9}$$

whereby ^{T} denotes the matrix transpose operator and (Arfken and Weber, 2005, Sec. 2.5)

$$\nabla = \vec{\mathbf{e}}_r \frac{\partial}{\partial r} + \vec{\mathbf{e}}_\beta \frac{1}{r} \frac{\partial}{\partial \beta} + \vec{\mathbf{e}}_\alpha \frac{1}{r \sin\beta} \frac{\partial}{\partial \alpha} \tag{10}$$

with

$$\vec{\mathbf{e}}_r = \begin{bmatrix} \cos\alpha \sin\beta \\ \sin\alpha \sin\beta \\ \cos\beta \end{bmatrix},\ \vec{\mathbf{e}}_\beta = \begin{bmatrix} \cos\alpha \cos\beta \\ \sin\alpha \cos\beta \\ -\sin\beta \end{bmatrix},\ \vec{\mathbf{e}}_\alpha = \begin{bmatrix} -\sin\alpha \\ \cos\alpha \\ 0 \end{bmatrix}.$$

Fig. 1 visualizes the unit vectors $\vec{\mathbf{e}}_r, \vec{\mathbf{e}}_\beta, \vec{\mathbf{e}}_\alpha$ of the coordinate dimensions. Recall that (r, β, α) denote the position $\vec{\mathbf{x}}$. The first vector on the right-hand side of (9) is the Cartesian form of $\vec{\mathbf{n}}$.

All of the above equations in this section need to be inserted into one another to establish the equivalents of (5) and (7) and consequently the equivalents of (3) and (4). Space restrictions prevent us from providing explicit expressions, and we can only state their components. Refer to Tab. 1 for the explicit expressions for the gradients in (10) expressed in SHs.

$P'_{n,|m|}(\cdot)$ in Tab. 1 and the factor $1/\sin\beta$ in (10) are not defined if they are evaluated at locations on the z-axis ($\beta = 0, \pi$). This is not a limitation so long as we choose the surface such that its normal at the locations where the surface intersects with the z-axis is parallel to the z-axis. Because then, the trigonometric functions in (9) vanish for those undefined cases.

References

George B. Arfken and Hans J. Weber. *Mathematical Methods for Physicists*. Elsevier, Amsterdam, 6 edition, 2005.

Ilya Balmages and Boaz Rafaely. Open-sphere designs for spherical microphone arrays. *IEEE TASLP*, 15(2): 727–732, 2007.

Benjamin Bernschütz. Microphone arrays and sound field decomposition for dynamic binaural recording. PhD thesis, Technische Universität Berlin, 2016.

A. J. Burton and G. F. Miller. The application of integral equation methods to the numerical solution of some exterior boundary-value problems. *Proc. of the Royal Soc. of London. A.*, 323(1553):201–210, 1971.

Nail Gumerov and Ramani Duraiswami. *Fast Multipole Methods for the Helmholtz Equation in Three Dimensions*. Elsevier, Amsterdam, 2005.

Edo Hulsebos, Diemer de Vries, and Emmanuelle Bourdillat. Improved microphone array configurations for auralization of sound fields by wave-field synthesis. *JAES*, 50(10):779–790, October 2002.

Jonathan Sheaffer, Maarten van Walstijn, Boaz Rafaely, and Konrad Kowalczyk. Binaural reproduction of finite difference simulations using spherical array processing. *IEEE/ACM Transactions on Audio, Speech, and Language Processing*, 23(12):2125–2135, 2015.

Bård Støfringsdal and Peter Svensson. Conversion of discretely sampled sound field data to auralization formats. *JAES*, 54(5):380–400, may 2006.

Mark R. P. Thomas. Practical concentric open sphere cardioid microphone array design for higher order sound field capture. In *ICASSP 2019 - 2019 IEEE International Conference on Acoustics, Speech and Signal Processing (ICASSP)*, pages 666–670, 2019.